Carbohydrate Polymers 93 (2013) 172–177

Contents lists available at SciVerse ScienceDirect

Carbohydrate Polymers

journal homepage: www.elsevier.com/locate/carbpol

Influence of TEMPO-oxidized cellulose nanofibril length on film properties

Hayaka Fukuzumi, Tsuguyuki Saito, Akira Isogai*

Graduate School of Agricultural and Life Sciences, The University of Tokyo, 1-1-1 Yayoi, Bunkyo-ku, Tokyo 113-8657, Japan

ARTICLE INFO

Article history:
Received 17 January 2012
Received in revised form 27 April 2012
Accepted 30 April 2012
Available online 18 May 2012

Keywords:
TEMPO
Cellulose nanofibril
Nanofibril length
Film properties
Oxygen permeability

ABSTRACT

Various mechanical disintegration conditions in water were applied to 2,2,6,6-tetramethylpiperidine-1-oxyl (TEMPO)-oxidized cellulose to prepare TEMPO-oxidized cellulose nanofibrils (TOCNs) of uniform widths ~4 nm but with three different average lengths, 200, 680, and 1100 nm. The viscosity average degrees of polymerization of the TOCNs were 250, 350, and 400, respectively. Self-standing TOCN and TOCN-coated poly(ethylene terephthalate) (PET) and poly(lactic acid) (PLA) films were prepared, and the optical, mechanical and gas-barrier properties of the films were evaluated in terms of nanofibril length. Only small differences in density, water content, and elastic modulus of the films were observed but TOCN films prepared from longer nanofibrils clearly showed higher tensile strengths, elongations at break and crystallinity indices. The oxygen barrier properties of the TOCN-coated PET and PLA films increased with increasing nanofibril length. In contrast, nanofibril length had almost no influence on water vapor-barrier properties.

1. Introduction

Crystalline nanofibrillated celluloses or nanocelluloses from 3 nm to 2 μm in width have attracted significant attention because they have potential applications as nano-reinforcing elements in polymer composites (Eichhorn et al., 2010), nano-filtration materials, rheology-control agents, hydro- and aero-gels with unique properties (Abe & Yano, 2011; Aulin, Netrval, Wågberg, & Lindström, 2010; Olsson et al., 2010; Pääkkö et al., 2008; Saito, Uematsu, Kimura, Enomae, & Isogai, 2011), and high gas-barrier films (Aulin, Gallstedt, & Lindström, 2010; Fukuzumi, Saito, Iwata, Kumamoto, & Isogai, 2009; Fukuzumi et al., 2011; Hult, Lotti, & Lenes, 2010; Isogai, Saito, & Fukuzumi, 2011; Siró, Plackett, Hedenqvist, Ankerfors, & Lindström, 2010; Spence, Venditti, Rojas, Habibi, & Pawlak, 2010; Syverud & Stenius, 2009). Nanocelluloses are produced from native wood or cotton cellulose fibers with or without pretreatment by mechanical disintegration in water, during which the numerous hydrogen bonds between the microfibrils in native cellulose fibers are partially or extensively cleaved to form cellulose microfibrils/nanowhiskers individually or in bundles.

Microfibrillated celluloses (MFCs) with 10–2000 nm widths have been manufactured from wood celluloses by high-shear mechanical homogenization in water (e.g. Henriksson, Henriksson, Berglund, & Lindström, 2007; Turbak, Snyder, & Sandberg, 1983; Siró & Plackett, 2010) and are commercially available as CELISH® (Daicel FineChem, Ltd., Japan). Cellulose nanowhiskers (CNWs) with 5–10 nm widths are produced from wood celluloses by hydrolysis with strong mineral acids (e.g. Dong, Revol, & Gray, 1998; Elazzouzi-Hafraoui et al., 2008; Marchessault, Morehead, & Walter, 1959). Other cellulose nanofibrils are prepared from native celluloses by 2,2,6,6-tetramethylpiperidine-1-oxy radical (TEMPO)-mediated oxidation and the subsequent mechanical disintegration of the oxidized celluloses in water (e.g. Isogai et al., 2011; Saito, Kimura, Nishiyama, & Isogai, 2007; Saito et al., 2009). Two important characteristics of TEMPO-oxidized cellulose nanofibrils (TOCNs) are: (1) TOCNs can be dispersed in water as almost completely individual fibrils with homogenous widths of 3–4 nm (Isogai et al., 2011) and (2) abundant sodium carboxylate groups are present on the crystalline cellulose fibril surfaces (~1.7 carboxylate groups nm^{-2}), by which electrostatic repulsion and/or osmotic behavior work effectively between the anionically charged TOCNs in water (Isogai et al., 2011; Okita, Saito, & Isogai, 2010).

Because individual TOCNs with 3–4 nm widths and high aspect ratios (>50) can be dispersed in water, highly transparent TOCN films can be prepared by aqueous TOCN dispersions on plates. Moreover, plastic films with thin TOCN layers can be prepared by coating an aqueous TOCN dispersion on surface-hydrophilized plastic base films. TOCN and TOCN-coated films have been studied in terms of optical, mechanical, thermal and gas-barrier properties (Fujisawa, Okita, Fukuzumi, Saito, & Isogai, 2011; Fukuzumi et al., 2009; Fukuzumi, Saito, Okita, & Isogai, 2010; Fukuzumi et al., 2011; Isogai et al., 2011). TOCN films have particularly high oxygen-barrier properties under dry conditions, although oxygen transmission rates clearly increase at high relative humidities (Fukuzumi et al., 2011).

* Corresponding author. Tel.: +81 3 5841 5538; fax: +81 3 5841 5269.
E-mail address: aisogai@mail.ecc.u-tokyo.ac.jp (A. Isogai).

0144-8617/$ – see front matter © 2012 Elsevier Ltd. All rights reserved.
http://dx.doi.org/10.1016/j.carbpol.2012.04.069

It has been reported that optical and mechanical properties of nanocellulose sheets are influenced by the degree of polymerization (DP), crystallinity and chemical composition of the celluloses used (Henriksson, Berglund, Isaksson, & Lindström, 2008). In the case of TOCNs, fibril length (and fibril length distribution) may be expected to influence optical, mechanical and gas-barrier properties to some extent. Although TOCNs prepared from wood celluloses have almost homogeneous widths (3–4 nm), their lengths and length distributions vary, depending on the preparation conditions, and the influence of these on film properties has not been studied in detail. The lengths of TOCNs can be controlled by the pH of the TEMPO-mediated oxidation system (Saito et al., 2009) or the amount of NaClO added in the TEMPO-mediated oxidation in water at pH 10 (Shinoda, Saito, Okita, & Isogai, 2012). In these cases, however, extensive changes in carboxylate content are unavoidable so the influence of fibril length alone on film properties cannot be extracted from the results.

In this study, therefore, we first prepared TEMPO-oxidized wood cellulose with a carboxylate content of 1.5 mmol g^{-1}, and various mechanical disintegration conditions were applied in water to prepare TOCNs with different nanofibril lengths. TOCN and TOCN-coated plastic films were prepared, and their optical, mechanical and gas-barrier properties were evaluated in terms of nanofibril length.

2. Materials and methods

2.1. Materials

A never-dried softwood bleached kraft pulp was used as the cellulose source for TEMPO-mediated oxidation. The pulp had a viscosity average DP (DP_v) of 1200, when 0.5 M copper ethylenediamine (cuen) was used as the solvent (Sihtola, Kyrklund, Laamanen, & Palenius, 1963). The pulp contained approximately 90% cellulose and 10% hemicelluloses. Laboratory grade TEMPO, sodium bromide, and 13% sodium hypochlorite solution (Wako Pure Chemicals, Co. Ltd., Tokyo, Japan) were used as received. TEMPO-oxidized cellulose was prepared from the softwood cellulose using the TEMPO/NaBr/NaClO system at pH 10 according to a previously reported method using NaClO at 5 mmol g^{-1}-cellulose (Saito et al., 2007). The TEMPO-oxidized cellulose thus prepared had a DP_v of 550 and a sodium carboxylate content of 1.5 mmol g^{-1}. Commercial poly(ethylene terephthalate) (PET) (Teijin DuPont Films, Japan), and poly(lactic acid) (PLA) films (Mitsui Chemical Tohcello, Inc., Japan) were used as coating substrates.

2.2. Preparation of TEMPO-oxidized cellulose nanofibrils (TOCNs)

An aqueous 0.15% slurry of the TEMPO-oxidized cellulose was subjected to blender-type homogenization at 15,000 rpm (Excel Auto ED-4, Nissei, Japan) for 5 or 10 min, and subsequently sonicated at 19.5 kHz and 300 W output power (26 mm probe tip diameter, US-300T, Nissei, Japan) for 2, 4 or 20 min (Table 1). Three transparent aqueous dispersions (TOCNs-A, -B, and -C) were obtained after centrifugation of the dispersions at 12,000 × *g* for 10 min to remove unfibrillated and partly fibrillated fractions. The yields of TOCNs after centrifugation are given in Table 1. The homogenization and sonication conditions for TOCN-C have been generally adopted in our laboratory to prepare longer TOCNs with less damage. The more harsh disintegration conditions for TOCNs-A and -B were selected in this study to prepare TOCNs in smaller and different length.

2.3. Preparation of TOCN films

Self-standing TOCN films ~10 μm in thickness were prepared by pouring the TOCN dispersions into polystyrene petri dishes and drying at 40 °C for 3 days. The TOCN films were easily detached from the dish after drying. TOCN-coated films ~1.5 μm in TOCN thickness were prepared as follows. The PET films (thickness 50 μm; area 9 cm × 9 cm) and PLA films (thickness 25 μm; area 9 cm × 9 cm) were surface-hydrophilized by plasma exposure at 5 mA for 5 min in vacuum using a soft-etching device (DSDE-AF, Meiwafosis Co., Ltd., Japan). The 0.15% TOCN/water dispersion (10 ml) was uniformly cast onto the hydrophilized surface of the base film and allowed to dry naturally at room temperature for 3 days.

2.4. Analyses

Freeze-dried TOCNs (0.5 g) were reacted with $NaClO_2$ (0.1 mmol) in an acetate buffer (50 ml) at pH 4.5 and room temperature for 2 days to selectively oxidize small amounts of C6-aldehydes to C6-carboxylates (Saito & Isogai, 2004; Shinoda et al., 2012). After subsequent conversion of carboxyl groups to sodium carboxylate groups using a diluted NaOH solution, the $NaClO_2$-oxidized TOCNs were purified and isolated by dialysis against water followed by freeze-drying. Freeze-dried samples (0.04 g) were dissolved in 0.5 M cuen and their viscosities measured using a capillary viscometer. The DP_v values of the $NaClO_2$-oxidized TOCNs were calculated from their intrinsic viscosities (Sihtola et al., 1963).

A 10 μl aliquot of 0.015% (w/v) TOCN/water dispersions was mounted on a glow-discharged carbon-coated electron microscopy grid and the excess liquid was absorbed by a filter paper. One drop of 1% uranyl acetate negative stain was added before drying and the excess solution was also removed with a filter paper. The stained TOCN dispersions were allowed to dry by natural evaporation. The sample grids were observed at 200 kV using a JEOL electron microscope (JEM 2000-EX, Tokyo, Japan). The sizes of TEM images were approximately 1 μm × 1.3 μm for TOCNs-A and -B, and 5 μm × 6.7 μm for TOCN-C.

The films were conditioned in desiccators at desired relative humidities for at least 48 h, and their weights measured at a resolution of ±2 μg. Dry weights of the films were measured after drying the films at 105 °C for 3 h followed by storage in desiccators with P_2O_5 for 3 h. Water contents of the self-standing TOCN films at various relative humidities under equilibrium conditions were calculated gravimetrically from the conditioned and dried weights. Fourier transform infrared (FT-IR) spectra of the TOCN films were recorded using a JASCO FT/IR-6100 spectrometer (Tokyo, Japan)

Table 1
Preparation conditions and properties of TOCNs.

	Homogenization time (min)	Sonication time (min)	Nanofibril yield (%)	Length-weighted average nanofibril length (nm)	DP_v[a]
TOCN-A	10	20	ca. 100	200	250
TOCN-B	10	4	98	680	350
TOCN-C	5	2	85	1100	400

[a] Viscosity-average degree of polymerization determined using 0.5 M cuen as the solvent during preparation.

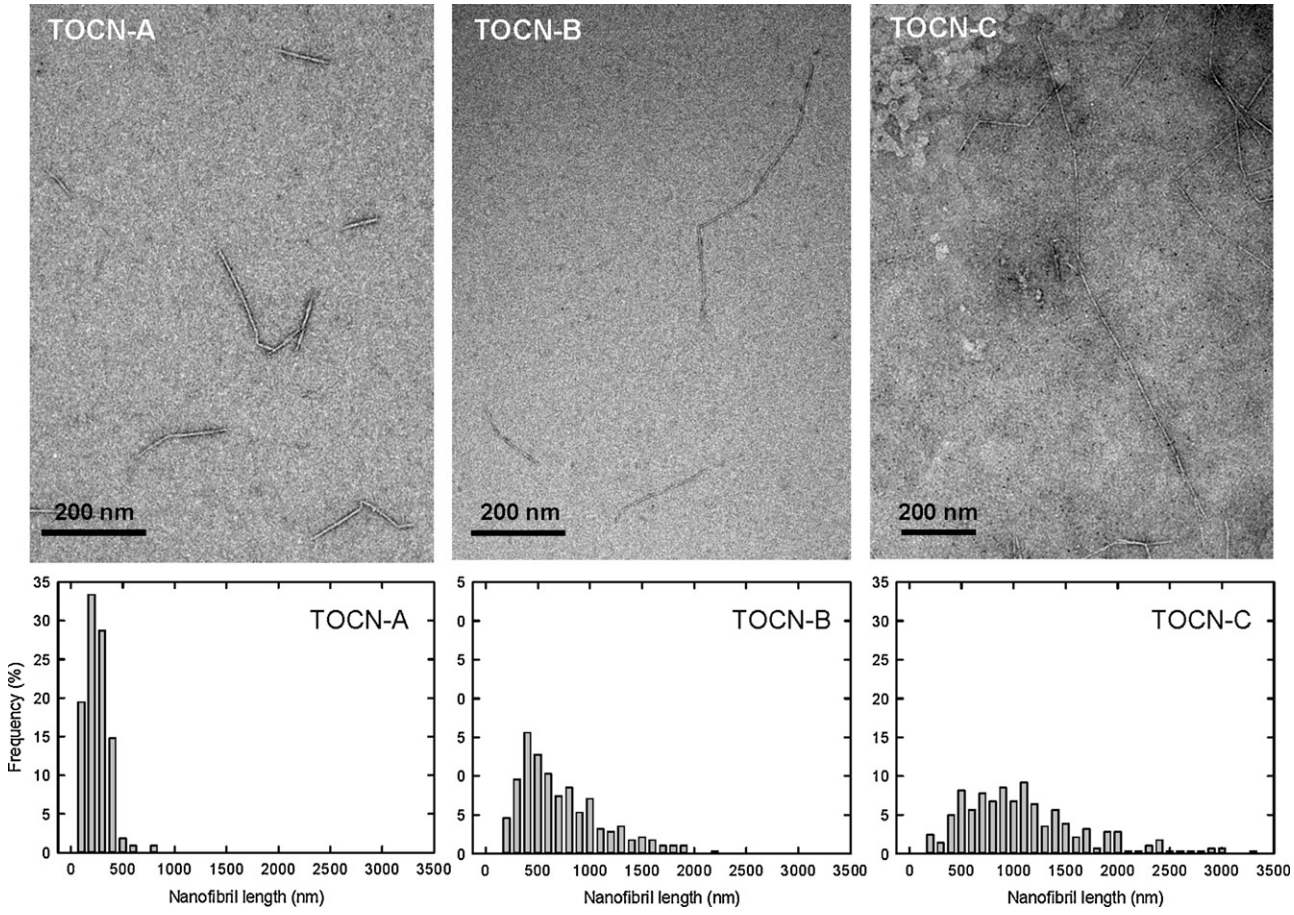

Fig. 1. TEM images of TOCN-A, TOCN-B and TOCN-C and their corresponding measured length distributions.

under transmission mode from 400 to 4000 cm^{-1} with a 4 cm^{-1} resolution. Crystallinity indices of cellulose I for the TOCN films were calculated from the IR spectra by the absorption ratios, A_{cryst} at 1372 cm^{-1}/A_{total} at 2900 cm^{-1} (Fig. S1 in Supplementary file) (Nelson & O'Connor, 1964). The light transmittance spectra of the TOCN/water dispersions and dried TOCN films were measured from 200 to 700 nm with a UV–vis–NIR spectrophotometer (JASCO, V-670, Japan). Film thicknesses of TOCN films and TOCN layers on the coated substrates were calculated from interference patterns that appeared in transmittance and/or reflectance spectra, using the JASCO analysis program according to a reported method (Lin & Chen, 2009). Refractive indices of 1.55, 1.65, and 1.49 were used for TOCN, PET and PLA, respectively, to calculate film thicknesses (Auras, Harte, & Selke, 2004; Isogai et al., 2011).

Tensile tests of self-standing TOCN films with ~10 μm thickness were carried out at 23 °C and 50% relative humidity (RH) using a Shimadzu EZ-TEST tensile tester (Tokyo, Japan) equipped with a 500 N load cell. Specimens with at least 20 mm length and 2 mm width were measured at 1.0 mm min^{-1} and a 10 mm span length, and at least 5 specimens were measured for each sample.

The PET and PLA films coated with TOCNs were subjected to oxygen permeability rate (OTR) determination at 23 °C and various RHs using an oxygen permeability testing apparatus (MOCON OX-TRAN 2/21, Modern Controls Inc., U.S.A.) according to a standard method (ASTM 3985). Each sample was conditioned in a desiccator at a desired RH for at least 12 h before measurement. The test areas were 50 and 5 cm^2 for films with low and high OTRs, respectively. Each sample was conditioned in the OTR system chamber for 3 h and the OTR was measured for more than 1 day until a stable value was obtained. Water vapor transmission rates (WVTRs) of the films were measured using a MOCON PERMATRAN-W 1/50 according to a standard method (ASTM 398). Flow upstream of the film was set at 10% RH, and the downstream varied from 40 to 100% RH. The WVTR value was measured for more than 1 h until a stable value was obtained.

3. Results and discussion

3.1. Nanofibril lengths and length distributions of TOCNs

The 0.15% (w/v) TOCN/water dispersions were transparent, and their flow behavior indicated that viscosities are in the order TOCN-C > TOCN-B > TOCN-A. TEM images of the TOCNs showed that the nanofibrils clearly differed in length, depending on the mechanical disintegration conditions, while they had almost uniform widths of 4 nm (Fig. 1). More than 200 nanofibrils on 50–100 TEM images for each TOCN sample were used to measure lengths and length distributions using Image-J software version 1.45. Any kinks present in individual nanofibrils were ignored for the length calculation; each length was measured as one connected TOCN, even though it had some kinks. The length distribution histograms were asymmetric and extended towards the longer part in a similar manner to those of cellulose nanowhiskers (Elazzouzi-Hafraoui et al., 2008). The length-weighted average lengths were 200, 680 and 1100 nm for TOCNs-A, -B, and -C, respectively. Thus, the length of TOCNs can be controlled by selecting the mechanical disintegration conditions of the TOCN/water slurry, while maintaining a uniform fibril width. The lengths of TOCN-A ranged from 50 to 750 nm. TOCN-B lengths ranged from 120 to 2100 nm, while TOCN-C had a much wide length distribution from 110 to 3600 nm. The sharp blades in the

blender-type homogenizer would mechanically cut the nanofibrils into various lengths.

Mechanical disintegration times and properties of the three TOCNs are listed in Table 1. Because almost complete individualization was achieved for TOCN-A, the nanofibril yield was almost 100%. The nanofibril yield for TOCN-C was 85% because it contained some unfibrillated and partly fibrillated fractions due to the short disintegration times used. The DP_v values of the TOCNs also decreased with decreasing average nanofibril length, showing that TOCN lengths are correlated to their DP_v values; the TOCN lengths become shorter in association with depolymerization.

3.2. Optical and mechanical properties of TOCN films

Light transmittances of self-standing TOCN films 10 μm in thickness are shown in Fig. 2A. All TOCN films had light transmittances of >80% at 600 nm, which are in good agreement with those previously reported (Isogai et al., 2011). The interference in the near-infrared region indicates high smoothness of the film surfaces and uniformity of the film thickness over large surface areas (Takahashi et al., 2009). The films prepared from TOCN-A had a slightly higher light transmittance than the others. The short nanofibrils of TOCN-A prepared by long mechanical disintegration times may have enabled high dispersibility in water. Thus, the light transmittance or dispersibility of TOCN in water, shown in Fig. 2B, corresponds well to the transparency of the self-standing TOCN films in Fig. 2A.

Typical stress–strain curves of the self-standing TOCN films are shown in Fig. 3. In particular, the tensile strength increased with increasing nanofibril length from TOCN-A to TOCN-C, in association with an increased elongation at break. The film densities, water contents at 23 °C and 50% RH, elastic moduli, tensile strengths, elongations at break, and crystallinity indices of the three TOCN films are listed in Table 2. These three TOCN films had quite similar densities of about 1.4 g cm^{-3} and water contents of ~12%, showing that the TOCN films have similarly hygroscopic and dense structures. In contrast, the TOCN films had higher tensile strength and greater elongation at break as the nanofibril length and DP_v increased, so these properties are strongly influenced by the nanofibril length.

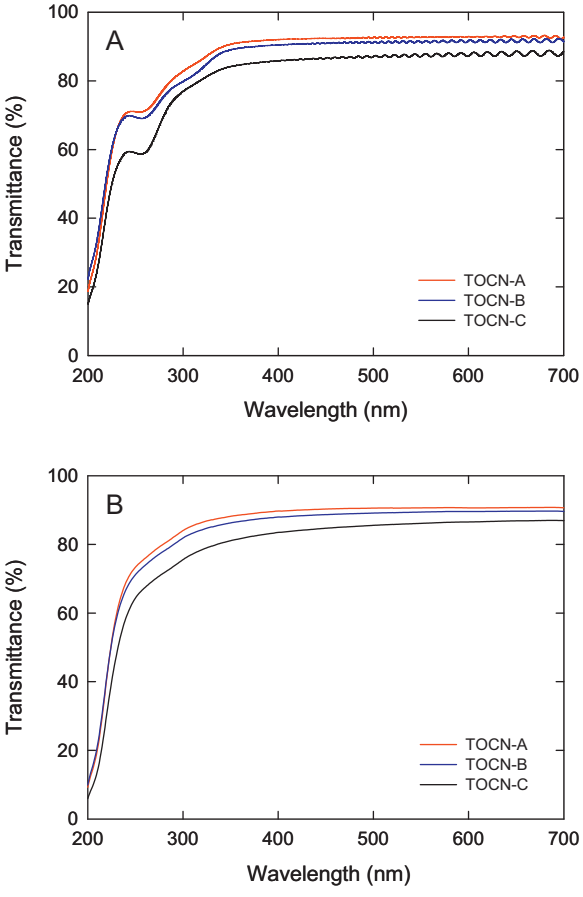

Fig. 2. UV–vis light transmittance spectra of self-standing TOCN films with 10 μm thickness (A) and 0.15% TOCN/water dispersions (B).

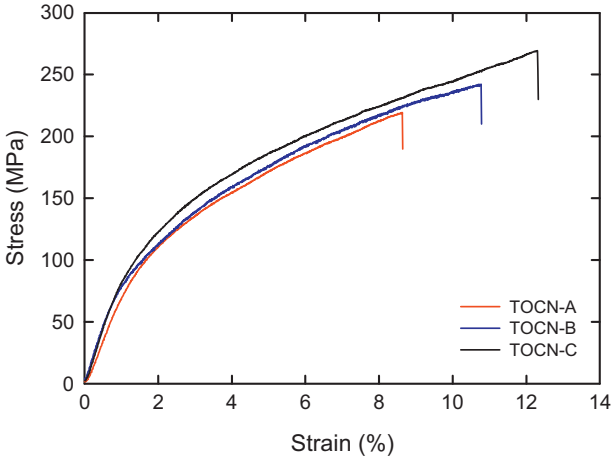

Fig. 3. Stress–strain curves of self-standing TOCN films during tensile test.

The higher elastic moduli of the TOCN-B and TOCN-C films may have been caused by their slightly higher film densities (Table 2) (Henriksson et al., 2008; Retegi et al., 2010). Elastic moduli of the TOCN films may also be correlated to their crystallinity indices (Iwamoto, Nakagaito, & Yano, 2007; Retegi et al., 2010). IR crystallinity indices of cellulose I for the self-standing TOCN films (Table 2) were determined from FT-IR spectra according to a previously reported method (Fig. S1 in Supplementary file) (Nelson & O'Connor, 1964). The IR crystallinity index increased with increasing nanofibril length, indicating that the higher elastic modulus and density and lower water content of the TOCN-C films are probably associated with the higher crystallinity index of cellulose I. The amount of disordered edges of nanofibrils may increase with decreasing nanofibril length through the longer mechanical disintegration times for the TEMPO-oxidized cellulose in water. Tensile strength and elongation at break of TOCN films substantially increased with nanofibril length. It was reported that increased DP causes higher elongations at break, associated with higher tensile strengths (Henriksson et al., 2008).

3.3. Oxygen and water vapor permeability rates of TOCN films

The OTRs of the TOCN-coated PET and PLA films under various RH conditions are shown in Fig. 4. OTRs of the base films were almost unchanged over the entire RH range due to their hydrophobic nature with the PET and PLA base films having high OTRs of ~30 and ~900 ml m^{-2} day^{-1} kPa^{-1}, respectively. On the contrary, the oxygen permeability of hydrophilic TOCN-coated films was strongly influenced by RH. The OTRs of TOCN-coated PET and PLA films were extremely low at 0% RH, while they exponentially increased with increasing RH. The OTR values at 35% RH increased approximately two orders of magnitude over that at 0% RH and approached the OTRs of the base films at 75% RH. TOCN-C showed the highest oxygen-barrier properties in the 0–50% RH range. The greatest differences between the three TOCNs clearly appeared at 0% RH but became smaller at 75% RH. Because the

Table 2
Properties of self-standing TOCN films. The density and water content of the films were measured at 23 °C and 50% relative humidity.

	Density (g cm^{-3})	Water content (%)	Elastic modulus (GPa)	Tensile strength (MPa)	Elongation at break (%)	Crystallinity index[a]
TOCN-A	1.40	12.2	8.8 ± 1.4	224 ± 25	8.9 ± 0.9	0.56
TOCN-B	1.42	12.3	9.4 ± 0.7	257 ± 22	9.0 ± 1.3	0.59
TOCN-C	1.43	11.6	9.8 ± 0.8	266 ± 10	9.9 ± 1.6	0.64

[a] Calculated from each IR spectrum by the absorption ratio, $A_{1372\ cm^{-1}}/A_{2900\ cm^{-1}}$ (Nelson & O'Connor, 1964).

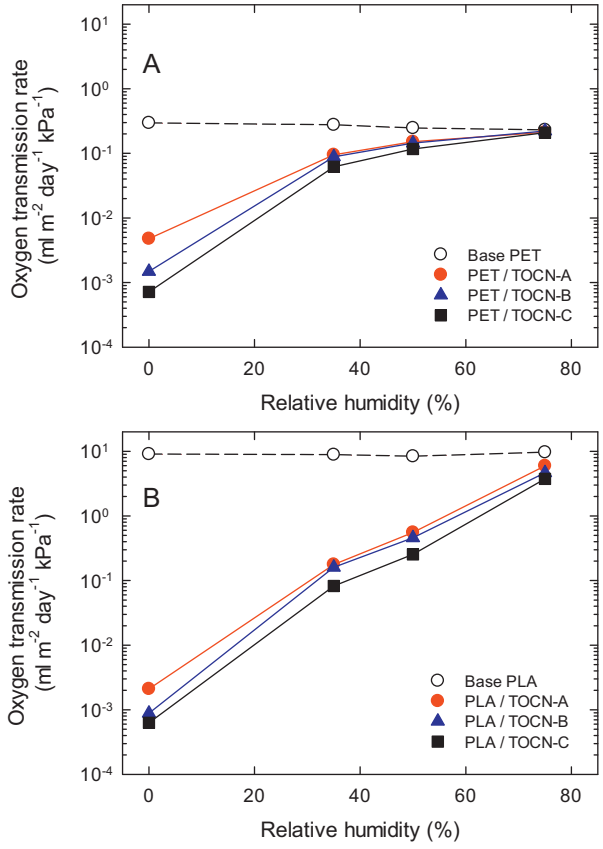

Fig. 4. Oxygen transmission rates of TOCN-coated PET (A) and PLA (B) films. The thicknesses of the PET and PLA base films were 50 μm and 25 μm, respectively. TOCN layers approximately 1.5 μm thick were coated on the base films.

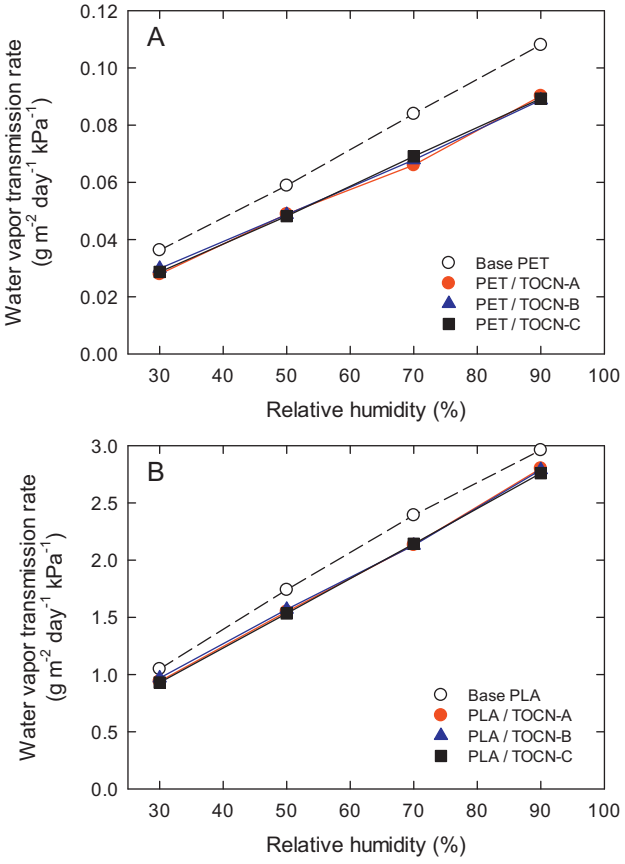

Fig. 5. Water vapor transmission rates of TOCN-coated PET (A) and PLA (B) films. See Fig. 4 for details of the base films and coating layers.

self-standing TOCN-C film had the highest crystallinity index, the high crystallinity of cellulose I in the film may have imparted the high oxygen-barrier properties. A similar result was reported when comparing oxygen permeability between microfibrillated cellulose and cellulose nanowhisker films with longer and shorter nanocellulose lengths, respectively (Belbekhouche et al., 2011).

On the contrary, the nanofibril length had almost no influence on the water vapor transmission rates (WVTRs) of the TOCN-coated films (Fig. 5). The WVTR increased linearly with increasing RH. This trend was similar to that of the base films but the WVTR values of the TOCN-coated films were lower than those of the base films at the same RH. This is probably due to the increased thickness of the TOCN-coated films. Fig. 6 shows the relationships between RH and water content of the self-standing TOCN films under equilibrium conditions. No significant difference in water content at each RH was observed between the three TOCN films, showing that the amounts of adsorbed water in the TOCN films at each RH were quite similar, regardless of nanofibril length. Although the self-standing TOCN films had a high water vapor permeability of approximately 70 g μm m^{-2} day^{-1} kPa^{-1} at 30% RH and this value increased exponentially with increasing RH (data not shown), the WVTRs could be suppressed to low values over the entire RH range,

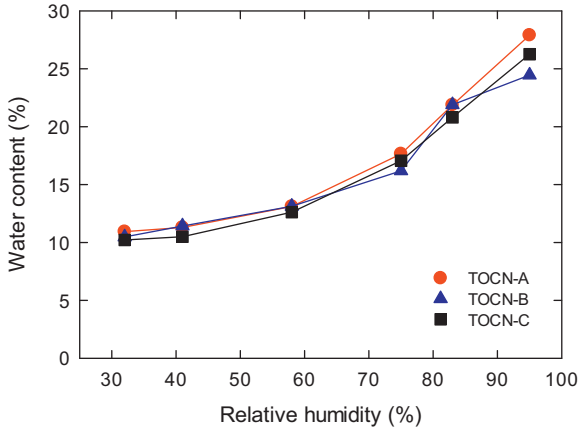

Fig. 6. Water content of TOCN films at 23 °C and various relative humidities under equilibrium conditions.

as shown in Fig. 5, by coating TOCNs on hydrophobic PET or PLA films. The hydrophilic nature of the TOCNs coated on hydrophobic base polymer films enables low OTRs and WVTRs even under high RH conditions.

4. Conclusions

The influence of TOCN length on optical, mechanical, and gas-barrier properties of TOCN films was investigated using TOCNs with three different nanofibril lengths. Shorter average TOCN lengths resulted in a lower DP_v and higher light transmittances for both TOCN/water dispersions and TOCN films. Only small differences were observed in density and water content at 23 °C and 50% RH between self-standing TOCN films prepared with differing nanofibril lengths. In contrast, a longer average TOCN length resulted in a higher tensile strength and elongation at break of TOCN films. The oxygen-barrier properties differed between the three TOCN-coated films, particularly at low RH. Longer nanofibril lengths produced higher oxygen-barrier properties. However, nanofibril length had almost no effect on water vapor barrier properties, which were primarily influenced by the water vapor transmission rates of the hydrophobic base films.

Acknowledgements

This research was supported by Grants-in-Aid for Scientific Research (Grants 21228007 and 21-6112) from the Japan Society for the Promotion of Science (JSPS). We would also like to thank Dr. Yoshiaki Kumamoto and Mr. Kenta Mukai (Kao Corporation) for providing commercial base films.

Appendix A. Supplementary data

Supplementary data associated with this article can be found, in the online version, at http://dx.doi.org/10.1016/j.carbpol.2012.04.069.

References

Abe, K., & Yano, H. (2011). Formation of hydrogels from cellulose nanofibers. *Carbohydrate Polymers*, *85*, 733–737.
Aulin, C., Netrval, J., Wågberg, L., & Lindström, T. (2010). Aerogels from nanofibrillated cellulose with tunable oleophobicity. *Soft Matter*, *6*, 3298–3305.
Aulin, C., Gallstedt, M., & Lindström, T. (2010). Oxygen and oil barrier properties of microfibrillated cellulose films and coatings. *Cellulose*, *17*, 559–574.
Auras, R., Harte, B., & Selke, S. (2004). An overview of polylactides as packaging materials. *Macromolecular Bioscience*, *4*, 835–864.
Belbekhouche, S., Bras, J., Siqueira, G., Chappey, C., Lebrun, L., Khelifi, B., et al. (2011). Water sorption behavior and gas barrier properties of cellulose whiskers and microfibrils films. *Carbohydrate Polymers*, *83*, 1740–1748.
Dong, X. M., Revol, J.-F., & Gray, D. G. (1998). Effect of microcrystallite preparation conditions on the formation of colloid crystals of cellulose. *Cellulose*, *5*, 19–32.
Eichhorn, S. J., Dufresne, A., Aranguren, M., Marcovich, N. E., Capadona, J. R., Rowan, S. J., et al. (2010). Review: Current international research into cellulose nanofibres and nanocomposites. *Journal of Materials Science*, *45*, 1–33.
Elazzouzi-Hafraoui, S., Nishiyama, Y., Putaux, J. L., Heux, L., Dubreuil, F., & Rochas, C. (2008). The shape and size distribution of crystalline nanoparticles prepared by acid hydrolysis of native cellulose. *Biomacromolecules*, *9*, 57–65.
Fukuzumi, H., Saito, T., Iwata, T., Kumamoto, Y., & Isogai, A. (2009). Transparent and high gas barrier films of cellulose nanofibers prepared by TEMPO-mediated oxidation. *Biomacromolecules*, *10*, 162–165.
Fukuzumi, H., Saito, T., Okita, Y., & Isogai, A. (2010). Thermal stabilization of TEMPO-oxidized cellulose. *Polymer Degradation and Stability*, *95*, 1502–1508.
Fukuzumi, H., Saito, T., Iwamoto, S., Kumamoto, Y., Ohdaira, T., Suzuki, R., et al. (2011). Pore size determination of TEMPO-oxidized cellulose nanofibril films by positron annihilation lifetime spectroscopy. *Biomacromolecules*, *12*, 4057–4062.
Fujisawa, S., Okita, Y., Fukuzumi, H., Saito, T., & Isogai, A. (2011). Preparation and characterization of TEMPO-oxidized cellulose nanofibril films with free carboxyl groups. *Carbohydrate Polymers*, *84*, 579–583.
Henriksson, M., Henriksson, G., Berglund, L. A., & Lindström, T. (2007). An environmentally friendly method for enzyme-assisted preparation of microfibrillated cellulose (MFC) nanofibers. *European Polymer Journal*, *43*, 3434–3441.
Henriksson, M., Berglund, L. A., Isaksson, P., & Lindström, T. (2008). Cellulose nanopaper structures of high toughness. *Biomacromolecules*, *9*, 1579–1585.
Hult, E. L., Lotti, M., & Lenes, M. (2010). Efficient approach to high barrier packaging using microfibrillar cellulose and shellac. *Cellulose*, *17*, 575–586.
Isogai, A., Saito, T., & Fukuzumi, H. (2011). TEMPO-oxidized cellulose nanofibers. *Nanoscale*, *3*, 71–85.
Iwamoto, S., Nakagaito, A. N., & Yano, H. (2007). Nano-fibrillation of pulp fibers for the processing of transparent nanocomposites. *Applied Physics A: Materials Science & Processing*, *89*, 461–466.
Lin, K., & Chen, Y. (2009). Improvement of electrical properties of sol–gel derived ZnO:Ga films by infrared heating method. *Journal of Sol–Gel Science and Technology*, *51*, 215–221.
Marchessault, R. H., Morehead, F. F., & Walter, N. M. (1959). Liquid crystal systems from fibrillar polysaccharides. *Nature*, *184*, 632–633.
Nelson, M. L., & O'Connor, R. T. (1964). Relation of certain infrared bands to cellulose crystallinity and crystal latticed type. Part II. A new infrared ratio for estimation of crystallinity in celluloses I and II. *Journal of Applied Polymer Science*, *8*, 1325–1341.
Okita, Y., Saito, T., & Isogai, A. (2010). Entire surface oxidation of various cellulose microfibrils by TEMPO-mediated oxidation. *Biomacromolecules*, *11*, 1696–1700.
Olsson, R. T., Azizi Samir, M. A. S., Salazar-Alvarez, G., Belova, L., Ström, V., Berglund, L. A., et al. (2010). Making flexible magnetic aerogels and stiff magnetic nanopaper using cellulose nanofibrils as templates. *Nature Nanotechnology*, *5*, 584–588.
Pääkkö, M., Vapaavuori, J., Silvennoinen, R., Kosonen, H., Ankerfors, M., Lindström, T., et al. (2008). Long and entangled native cellulose I nanofibers allow flexible aerogels and hierarchically porous templates for functionalities. *Soft Matter*, *4*, 2492–2499.
Retegi, A., Gabilondo, N., Peña, C., Zuluaga, R., Castro, C., Gañan, P., et al. (2010). Bacterial cellulose films with controlled microstructure-mechanical property relationships. *Cellulose*, *17*, 661–669.
Saito, T., & Isogai, A. (2004). TEMPO-mediated oxidation of native cellulose. The effect of oxidation conditions on chemical and crystal structures of the water-insoluble fractions. *Biomacromolecules*, *5*, 1983–1989.
Saito, T., Kimura, S., Nishiyama, Y., & Isogai, A. (2007). Cellulose nanofibers prepared by TEMPO-mediated oxidation of native cellulose. *Biomacromolecules*, *8*, 2485–2491.
Saito, T., Hirota, M., Tamura, N., Kimura, S., Fukuzumi, H., Heux, L., et al. (2009). Individualization of nano-sized plant cellulose fibrils by direct surface carboxylation using TEMPO catalyst under neutral conditions. *Biomacromolecules*, *10*, 1992–1996.
Saito, T., Uematsu, T., Kimura, S., Enomae, T., & Isogai, A. (2011). Self-aligned integration of native cellulose nanofibrils towards producing diverse bulk materials. *Soft Matter*, *7*, 8804–8809.
Shinoda, R., Saito, T., Okita, Y., & Isogai, A. (2012). Relationship between length and degree of polymerization of TEMPO-oxidized cellulose nanofibrils. *Biomacromolecules*, *13*, 842–849.
Siró, I., Plackett, D., Hedenqvist, M., Ankerfors, M., & Lindström, T. (2010). Highly transparent films from carboxymethylated microfibrillated cellulose: The effect of multiple homogenization steps on key properties. *Journal of Applied Polymer Science*, *119*, 2652–2660.
Siró, I., & Plackett, D. (2010). Microfibrillated cellulose and new nanocomposite materials: A review. *Cellulose*, *17*, 459–494.
Sihtola, H., Kyrklund, B., Laamanen, L., & Palenius, I. (1963). Comparison and conversion of viscosity and DP-values determined by different methods. *Paperi ja Puu*, *45*, 225–232.
Spence, K. L., Venditti, R. A., Rojas, O. J., Habibi, Y., & Pawlak, J. J. (2010). The effect of chemical composition on microfibrillar cellulose films from wood pulps: Water interactions and physical properties for packaging applications. *Cellulose*, *17*, 835–848.
Syverud, K., & Stenius, P. (2009). Strength and barrier properties of MFC films. *Cellulose*, *16*, 75–85.
Takahashi, M., Iyoda, K., Miyauchi, T., Ohkido, S., Tahashi, M., Wakita, K., et al. (2009). Preparation and characterization of Eu:Ti codoped $LiNbO_3$ films prepared by the sol–gel method. *Journal of Applied Physics*, *106*, 044102.
Turbak, A. F., Snyder, F. W., & Sandberg, K. R. (1983). Microfibrillated cellulose, a new cellulose product: Properties, uses, and commercial potential. *Journal of Applied Polymer Science Applied Polymer Symposia*, *37*, 815–827.